Exploiting Spatiotemporal Correlation for Wireless Networks Under Interference

Song Min Kim, Shuai Wang, and Tian He

***Abstract*— This paper starts from an empirical observation on the existence of spatiotemporal correlation among nearby wireless links within short time intervals. The phenomenon due to correlated interference has become pervasive with densely deployed wireless devices, causing potential errors in existing popular metrics built upon the assumption of link independence. To this end, we propose correlated ETX (cETX), which generalizes the widely-adopted ETX to maintain the accuracy under correlated links. To the best of our knowledge, this is the first work to introduce a unified metric embracing both temporal and spatiotemporal correlations. As a generalized metric, the highlight of our work is the broad applicability and effectiveness–extensive evaluations on ZigBee (802.15.4) and Wi-Fi (802.11b/g/n) testbeds deployed in a lab, corridor, and on a bridge reveal that: simply replacing ETX with cETX: 1) cuts down the error by 62.1%–70.2% and 2) saves averages of 22% and 37% communication cost in three unicast and nine broadcast protocols, respectively, under only 0.7% additional overhead.**

***Index Terms*— Wireless routing, route metrics, energy efficiency.**

I. Introduction

PACKET losses and corruptions are inevitable in wireless networks, where they inherently suffer from noise and interference [17], [21], [40], [41], [50]. To effectively utilize unreliable wireless links, research calls for metrics that can accurately estimate the qualities of individual links as well as end-to-end paths. Among the extensive volume of admirable studies dealing with routing under lossy links [9], [12], [49], expected transmission count (ETX) [12] is the most popular for its generality and effectiveness, and has been cited over 3,000 times according to Google Scholar.

Our further studies on link characteristics, however, reveal that ETX suffers from a few limitations. First, recent work on the temporal property of wireless links [11], [37] shows that transmissions over a link within a short time interval are highly dependent, indicating the existence of temporal correlation among transmissions. This property is not taken into account in the design of the ETX metric, imposing a limitation on its ability to reflect the true link quality. This is because ETX is defined as the inverse of packet reception ratio (PRR). This value is in fact the mean of the geometric random variable with independent trials, indicating that ETX is implicitly built on the independence assumption among transmissions.

Another link characteristic enlightened by current work [33], [38] is the existence of reception correlation among receivers of broadcast packets due to cross-network interference and correlated shadowing; The receptions of broadcast packets at adjacent nodes are correlated at the same time instant, indicating spatial correlation. In this work, we observe that spatial correlation interplays with temporal correlation to exhibit reception correlation at consecutive links. In other words, there exists spatiotemporal correlation, i.e., the packet reception of a link is dependent on the recent reception at preceding links along a path. Since existing metrics including ETX are hop-by-hop designs, they fail to take spatiotemporal correlation into account.

In this paper, we first reveal why ETX cannot represent the true quality of links in the face of temporal and spatiotemporal correlation. Then, to address this issue, we design an enhanced version of ETX, called correlated ETX (cETX) that explores the phenomena to reflect the true performance of links and paths more precisely compared to ETX. In detail, we provide a unified metric embracing both temporal and spatiotemporal correlation factors. While keeping the intuitive idea of ETX intact (i.e., explicitly quantifying expected number of transmissions), our metric selects better links and paths that leads to less transmissions, thus achieving energy savings. In summary, our contributions are as follows:

- We experimentally reveal the phenomenon of spatiotemporal correlation and its potential impact on routing designs.
- We propose a new metric – cETX, capable of capturing temporal and spatiotemporal properties of wireless links. To the best of our knowledge, this is the first work to embed the two effects into a unified metric.
- We demonstrate how to incorporate cETX into (i) classical shortest path unicast algorithms and (ii) classical/collaborative broadcast algorithms, while maintaining the unicast path optimality and minimizing network-wide broadcast overhead distributively.
- We compare the accuracy of cETX and ETX through ZigBee and Wi-Fi testbed experiments, and via analysis on the Roofnet [3] trace to demonstrate error reduction of 70.2%, 62.1%, and 33.2%, respectively.

Manuscript received July 19, 2016; revised May 9, 2017; accepted June 24, 2017; approved by IEEE/ACM TRANSACTIONS ON NETWORKING Editor J. Xie. Date of publication August 11, 2017; date of current version October 13, 2017. This work was supported in part by the National Science Foundation under Grant CNS-1525235, Grant CNS-1444021, Grant CNS-1717059, and Grant CNS-1718456. A conference paper [25] containing preliminary results of this paper appeared in ACM SenSys 2015. *(Corresponding author: Tian He.)*

S. M. Kim is with the Department of Computer Science, George Mason University, Fairfax, VA 22030 USA (e-mail: song@gmu.edu).

S. Wang and T. He are with the Department of Computer Science and Engineering, University of Minnesota, Minneapolis, MN 55455 USA (e-mail: shuaiw@cs.umn.edu; tianhe@cs.umn.edu).

Digital Object Identifier 10.1109/TNET.2017.2732238

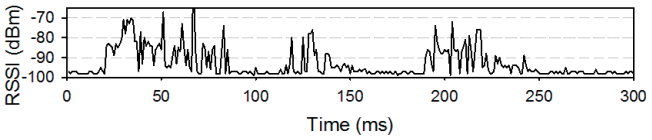

Fig. 1. Interference Burst.

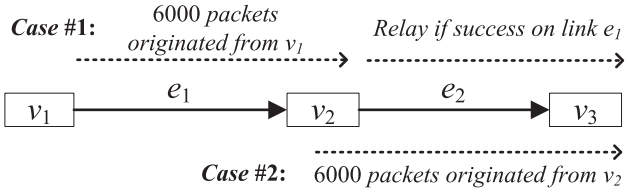

Fig. 2. Topology for spatiotemporal correlation experiment.

- We experimentally validate the applicability and effectiveness of cETX by replacing ETX with cETX in three unicast and nine broadcast protocols utilizing diverse network structures. cETX cuts down averages of 22% and 37% communication cost at the price of only 0.7% additional overhead via parameter piggybacking.

The paper is organized as follows. Section II motivates the work. Section III follows with the underlying model and reasoning. Section IV and Section V present the design and implementation of cETX, where its applications are introduced in Section VI. Section VII evaluates cETX, followed by in-situ deployment demonstration in Section VIII. We summarize related work in Section IX and conclude in Section X.

II. Motivation

Spatiotemporal correlation, or dependency between packet receptions in nearby links within a short time, is caused by interference and shadowing spanning through multiple links and last for a duration of multiple packets. Figure 1 shows the interference captured under an office environment where many of the spike bursts last over tens of milliseconds. The captured signal strength ranges from -70 to -90dBm, a level of typical Wi-Fi signals. Wi-Fi interference data collected during the day in the university building indicates that the bursty interference extends up to $29ms$, where the silent durations in between interference are mostly (90.6%) shorter than $22ms$. In sum, the observed interference from Wi-Fi is not only explosive, but also strong enough to simultaneously affect multiple low-power 802.15.4 links, suggesting that it is one of the causes of spatiotemporal correlation.

A. Spatiotemporal Correlation Revealed

We experimentally validate the phenomenon of spatiotemporal correlation in practice, among consecutive wireless links along a path. A simple two-hop network is formed as shown in Figure 2, operating on 802.15.4 channel 12 with a transmission power of -25dBm. Ten such networks are deployed for statistical significance. In each network, two cases are tested. **Case #1:** Node v_1 transmits 6000 packets to v_2. Upon successfully receiving a packet, v_2 *relays* the packet to v_3 five times, each after 2, 8, 14, 20, and $26ms$ delay. **Case #2:** Node v_2 transmits 6000 packets generated by itself to v_3. Please note

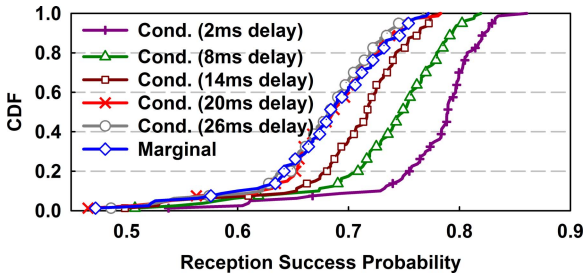

Fig. 3. Validating spatiotemporal correlation: whenever v_2 successfully receives a packet from v_1 it *relays* the packet five times to v_3 with different delays after reception. Thus, the success ratio of the relayed packets are *conditional* to the success of the transmission from v_1 to v_2, whereas the packets originated at v_2 are *marginal*.

Link1:	F	S	S	F	S	F	F	S	F	S
Link2:	F	F	F	S	S	S	F	F	S	S
	t_0	t_1	t_2	t_3	t_4	t_5	t_6	t_7	t_8	t_9

Fig. 4. Temporal correlation effect: Despite the same reception ratios, bursty failure in Link2 demands 1.9 transmissions where Link1 requires 1.6.

that, in case #1, transmission over link e_2 only occurs upon success on e_1. Therefore the reception success probability on e_2 in this case is conditional, given the success on preceding link e_1. On the other hand, the success probability over e_2 in case #2 is considered marginal, as it is irrelevant to e_1.

Figure 3 shows the experiment results of e_2's reception success probabilities, where conditional curves are obtained from case #1, and the marginal is from case #2. There exists a significant difference between the conditional probability with $2ms$ delay and the marginal probability. This supports the existence of spatiotemporal (positive) correlation between e_1 and e_2. That is, success on the preceding link (e_1) strongly implies success on the following link (e_2). Moreover, 20 and $26ms$ curves nearly overlap with the marginal curve, indicating spatiotemporal correlation fades away after $20ms$. To conclude, the experiment result gives us a simple but effective design guidance: We can increase the chance of a successful reception of a packet by simply relaying it within a short time interval, e.g., within $20ms$ in our experiment. We note that this aligns with our previous experimental result where the silent durations under bursty Wi-Fi interference are mostly $< 22ms$, showing that the Wi-Fi interference is a major cause of the spatiotemporal correlation.

B. Impact of Temporal Correlation

We illustrate the effect of temporal correlation via a simple example in Figure 4. In the history of ten transmissions of two links, S and F represent transmission success and failure. Since both links experience five S and five F, ETX indicates that the two links have equal performance, i.e., $10/5 = 2$ expected transmissions. However, the true average transmissions are not equal. Let's consider the case where we start transmitting at t_0. On Link1, the transmission succeeds at t_1 which causes two transmissions (i.e., fail at t_0, success at t_1). It costs four on Link2 as it succeeds at t_3 after three failures. Similarly, when we start the transmission at t_1, Link1 succeeds in a single transmission, while Link2 requires three.

Fig. 5. Temporal Correlation in real trace forces two links with similar reception ratios to exhibit different demands of 2.05 and 2.98 transmissions.

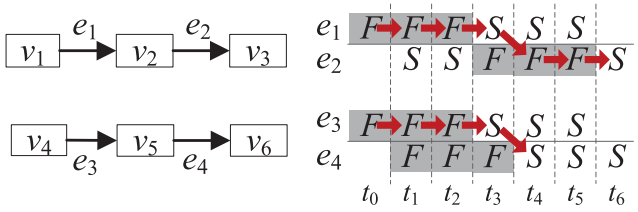

Fig. 6. Higher spatiotemporal correlation in consecutive links allows a better chance of success on the succeeding link following the link proceeding it. Marked with arrows, the number of transmissions for an end-to-end delivery is therefore smaller for the lower path.

When the start of a transmission occurs with equal probabilities across $t_0 - t_9$, we obtain the true average number of transmissions by repeating the above process up to t_9 and taking the average. This yields $(2+1+\cdots+1)/10 = 1.6$ and $(4+3+\cdots+1)/10 = 1.9$ for Link1 and Link2, indicating that Link1 is indeed a better link, despite their equal ETX. The performance difference of the two links can be described via conditional probability of failure followed by success, i.e, $Pr(S^n|F^{n-1})$ for $1 \leq n \leq 9$. This represents the link's ability to recover from failures. Thus, larger value indicate better performance. The values are 0.8 and 0.4 for Link1 and Link2, which confirms our argument.

The observation is further verified on the real traces in Figure 5, collected from two pairs of MICAz nodes. Each trace from two links holds a record of 10^3 packet transmissions. Black bars indicate failures while whites indicate successes. The packet reception ratios of Link3 and Link4 are 0.49 and 0.5, leading to approximately the same ETX of 2 for both links. However, the difference in the true average transmissions is quite large; 2.05 and 2.98 for Link3 and Link4, respectively. This is due to the consecutive failure chunks demonstrated in Link4; it is less able to recover from the failure than Link3. This difference again can be represented by the conditional probability. The values of $Pr(S^n|F^{n-1})$ are 0.49 and 0.29 for Link3 and Link4.

C. Impact of Spatiotemporal Correlation

In Figure 6, we use two two-hop paths to show how spatiotemporal correlation affects the network performance that ETX fails to capture. The packet reception ratios of every link in the figure, e_1-e_4, are equally 1/2. This yields ETX value of $2+2=4$ for both upper and lower paths. However, the links in the lower path, e_3 and e_4, are more positively correlated to each other than those (e_1 and e_2) in the upper path. Starting with the upper path, suppose that node v_1 has a packet to deliver to node v_3 and starts sending at time t_0. The packet successfully reaches v_2 after four transmissions (i.e. F→F→F→S). The transmission on e_2 starts at t_4 but succeeds at t_6, consuming three transmissions (F→F→S).

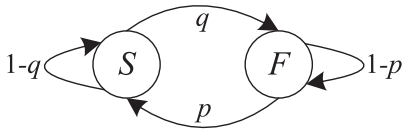

Fig. 7. Gilbert Model.

Therefore, end-to-end delivery in the upper path consumes a total of seven transmissions. This forwarding flow is demonstrated in Figure 6 as arrows. Similarly, we can easily see that the lower path requires five transmissions. This indicates that the lower path performs better than the upper path, despite their equivalence in the ETX values.

This example suggests that spatiotemporal correlation can improve the network performance. That is, when consecutive links in a path are strongly (positively) correlated, forwarding a packet shortly after receiving it from the preceding link has a high chance of successful receptions in the following link. Therefore, spatiotemporal correlation should be considered for an accurate performance measurement in multi-hop scenarios. To do so, we represent the degree of spatiotemporal correlation with conditional probability, i.e., $Pr(S_i^n|S_{i-1}^{n-1})$ at arbitrary time t_n when e_{i-1} precedes e_i. To verify, the conditional probability in this example yields $0.33 = Pr(S_2^n|S_1^{n-1}) < Pr(S_4^n|S_3^{n-1}) = 1$, correctly reflecting the relative performance of the two paths under spatiotemporal correlation.

III. Design Background

This section first presents the model that lays the foundation of our design, followed by empirical evidences and analysis on the suitability of such a model for our purpose of capturing correlation.

A. Underlying Model

Here we present the underlying model to help understand our design discussed in the next section. Recall in section II we showed that both temporal and spatiotemporal correlations can be quantified by conditional probabilities. A simple way of modeling with conditional probabilities is the Markov representation. Our design starts off from the *Gilbert Model* [16] in Figure 7, a famous channel model based on two state Markov chain. In the model, S indicates error-free state, while F is when the channel is erroneous. The state transition probabilities are denoted as p and q. That is, by letting $Pr(F^n)$ and $Pr(S^{n-1})$ denote the probabilities of being at states F and S at times t_n and t_{n-1} respectively, then $p = Pr(S^n|F^{n-1})$. Similarly, $q = Pr(F^n|S^{n-1})$. Moreover, steady state probabilities of the two states are computed as

$$\pi_S = \frac{p}{p+q}, \pi_F = \frac{q}{p+q} \quad (1)$$

where they indicate the chance of being at the corresponding state at an arbitrary time instant regardless of the initial state, after a sufficient number of state transitions. We follow this model to represent status of a single link. That is, a transmission over the link succeeds if and only if the link is in state S, while fails in state F. This lets transition probabilities, p and q, to indicate temporal correlation within the link. Extending the

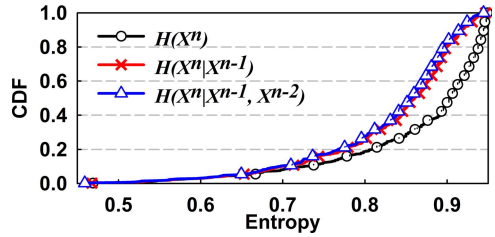

(a) Under Temporal Correlation

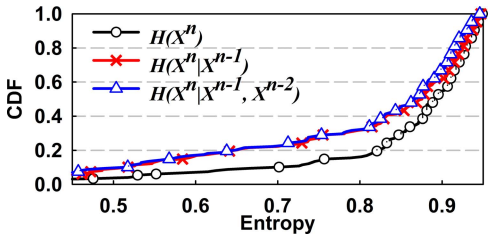

(b) Under Spatiotemporal Correlation

Fig. 8. Residual entropies in both (a) and (b) suggest that estimation on correlated links can benefit from 1^{st} order Markov chain design, while a higher order model is not necessary.

model to capture spatiotemporal correlation will be discussed later in Section IV.

B. Validity of 1st Order Markov Design

Our design is based on the Gilbert Model which is a first-order Markov model. In other words, the design benefits from the success/failure information obtained from the previous transmission to infer success of the following transmission. This raises a natural follow-up question: Can we even better estimate the success/failure of the next transmission, given the information on the last two, or even three transmissions? In other words, will a higher order Markov model help to further improve the quality of estimation? To this end, we analyze experimental data to show that the first order Markov model is the right choice; adopting higher order models will not make noticeable differences, while imposing additional complexity to the design and computation.

We achieve this by applying the concept of *entropy* from the information theory, which quantifies the uncertainty within a random variable as number of bits. Higher bit indicates higher uncertainty, which leads to lower estimation quality. Let X^n be a bernoulli random variable indicating reception success or failure at an arbitrary time instant, t_n. Then, the entropy within X^n is denoted as $H(X^n)$, indicating the marginal entropy. We further let X^{n-1} and X^{n-2} indicate reception success or failure at t_{n-1} and t_{n-2}, respectively (i.e., one and two time instants preceding X^n). Then, the conditional entropy expresses the amount of uncertainty in X^n when the value of X^{n-1} or both X^{n-1} and X^{n-2} are known, denoted as $H(X^n|X^{n-1})$ and $H(X^n|X^{n-1}, X^{n-2})$. For brevity we omit entropy computations which can be found in our work of [25].

Since success or failure can be expressed in a single bit, the maximum uncertainty is 1, when we do not have any clue on success or failure. Conversely, the uncertainty of 0 is when it can be perfectly estimated. Figure 8 shows marginal and conditional entropies in the face of two correlations. Figure 8(a) was obtained from experimental data of 5×10^5 consecutive packets over 50 links with packet interval of $6ms$, where experiment in Figure 8(b) was done similarly to that in Section II-A. While achieving the entropy of 0 is impossible due to natural randomness in links caused by shadowing and multipath fading, two clear observations can be made from the figures: (i) The gaps between conditional and marginal entropies indicate that the knowledge on previous transmission is helpful in estimating the success or failure of the following transmission, again verifying the existence of spatiotemporal and temporal correlations. (ii) $H(X^n|X^{n-1})$ and $H(X^n|X^{n-1}, X^{n-2})$ are very close in both figures, suggesting 1st order is as good as higher order design in the estimation quality, despite its lower complexity. This supports the effectiveness and sufficiency of our 1st order Markov-based design.

IV. Main Design

From the previous section we have learned that Gilbert Model successfully serves as our basis. However, the model is only capable of representing the status of a single link. In other words, it is insufficient to express spatiotemporal correlation, which is a relationship across multiple links. In this section, we address this issue by proposing an extended model, from which our metric cETX is derived.

A. Design Overview

As a generalized extension of ETX, cETX inherits the main idea of ETX to represent link quality by the expected number of transmissions. It is shown later in this section that cETX also retains the additive property of ETX, such that the path cost is simply the sum of cETX. Nevertheless, unlike ETX which assumes the packet receptions are independent, we take both temporal and spatiotemporal correlations into account to more accurately estimate the link/path cost. In fact, cETX is a generalized version of ETX, extended to incorporate knowledge on any degree of correlation into the link/path cost. For example, cETX simply reduces to ETX when there is no correlation among links.

B. Extended Gilbert Model

We propose an extended representation of the Gilbert Model for a few distinctive features that the original model does not possess. Specifically, it enables (i) the straightforward model extension to multi-hop scenarios, (ii) tracking the packet forwarding status to allow the computation of cETX directly from the model, and (iii) capturing spatiotemporal correlation among consecutive links in a path.

The Extended Gilbert Model describes the forwarding status of each packet in the form of 1^{st} order Markov chain. For ease of understanding we start from a single-hop network and its corresponding model depicted in Figure 9. The three states, S_1, F_1, and I, express packet forwarding on e_1. States S_1 and F_1 indicate the success and failure of the transmission over e_1, while I stands for the initial state indicating that the transmission has not yet taken place. Then, the packet forwarding process on the model follows intuitive

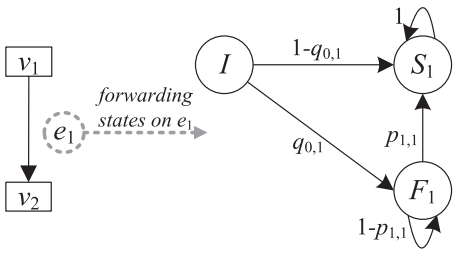

Fig. 9. A single-hop network (left) and the corresponding extended Gilbert Model representation (right). The model enables direct computation of our metric as well as straight-forward adaption to multi-hop scenario.

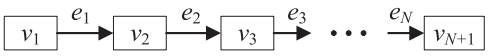

Fig. 10. N-hop Linear Network.

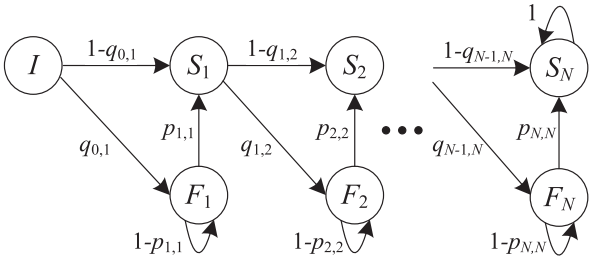

Fig. 11. N-hop Gilbert Model.

steps: starting from state I, a transition to either S_1 or F_1 occurs depending on the transmission success or failure. Upon failures, retransmission attempts are made to transit from F_1 to S_1, until S_1 is reached.

From the definition of state I, it is clear that its initial probability is 1. Now let us describe the transition probability introduced in the model. Keeping notations consistent to the previous sections, let S_1^n and F_1^{n-1} denote the transmission success and failure over e_1 at time t_n and t_{n-1}, respectively. Then, $p_{1,1}$ denotes the probability of a successful transmission after a failure in the previous time instant, $p_{1,1} = Pr(S_1^n|F_1^{n-1})$. Note that the subscript $_{1,1}$ used in $p_{1,1}$ denotes these two transmissions occur on the same link, e_1. Essentially $p_{1,1}$ represents the temporal correlation between consecutive transmissions within e_1. On the contrary, $q_{0,1}$ simply indicates the probability of failure in the initial transmission over e_1. Zero in the subscript implies that no previous transmission exists. Because we do not retransmit a packet that has already been received, the transition probability from S_1 to any other state is 0. In other words, the forwarding process over link e_1 terminates once S_1 has been reached.

C. Multi-Hop Gilbert Model

In the previous section we proposed the extended Gilbert Model for a single-hop network. We now further expand the model to a multi-hop scenario depicted in Figure 10.

The multi-hop Gilbert Model for the corresponding network is given in Figure 11, where it is an extension from the model in Figure 9 to express multiple links. As shown in the figure, the extension is as simple as adding a pair of S and F states per link. Then, the spatiotemporal parameter is introduced between consecutive links. In the multi-hop path once a successful transmission takes place in the preceding link, an immediate transmission follows in the next link. For instance, v_2 starts its transmission over e_2 shortly after the transmission success from v_1 to v_2 over e_1. The dependency between these two consecutive events is spatiotemporal correlation, which can be represented as $q_{1,2} = Pr(F_2^n|S_1^{n-1})$ where the subscript $_{1,2}$ on $q_{1,2}$ denotes that success at previous time t_{n-1} occurred on e_1, where the following failure was on e_2. Generally, spatiotemporal dependency is considered between any two consecutive links, indicated as $q_{i-1,i}$ for $2 \leq i \leq N$ in the multi-hop Gilbert Model. Clearly the multi-hop model captures both temporal and spatiotemporal correlation via p and q parameters.

The Rationale Behind the Model: The model enables precise estimation of link performance by capturing temporal and spatiotemporal correlations. Let us first look into how reflecting spatiotemporal correlation can achieve this goal, by again considering consecutive links e_1 and e_2 in a multi-hop packet forwarding scenario. Since the transmission (i.e., packet forwarding) on e_2 occurs iff. the transmission on e_1 was successful, the chance of success on e_2 can be precisely expressed with conditional probability, given that the transmission on e_1 was successful immediately before – i.e., $Pr(S_2^n|S_1^{n-1}) = q_{1,2}$. Depending on the degree of spatiotemporal correlation, this could be vastly different from the marginal probability (i.e., $Pr(S_2)$), as seen in Section II-A. Similarly, retransmission on e_2 occurs iff. previous transmission on the link has failed, indicating that considering temporal correlation (i.e., $Pr(S_2^n|F_2^{n-1}) = p_{2,2}$) enables precise performance measurement.

D. cETX Computation

We now show how our metric cETX can be computed from the multi-hop model in Figure 11. Note that cETX over a link is defined as the estimated number of transmissions to deliver a packet over the link. Suppose we want to compute cETX for an arbitrary link, $cETX_{e_i}$. Transmission on e_i starts on state S_{i-1}, and ends when S_i has been reached (I and S_1 for e_1). Since the state transition occurs for every transmission, the cETX$_{e_i}$ value equals the expected number of transitions to reach state S_i from S_{i-1}. This is often referred to as the expected first passage time in Markov chain theory, which can be computed as follows:

$$cETX_{e_i} = 1 + q_{i-1,i} \times \frac{1}{p_{i,i}} \tag{2}$$

The equation can be intuitively understood by referring to our model. The first term in Eq.(2), i.e., 1, indicates the initial transmission which is mandatory. The second term indicates the product of the initial transmission failure probability, i.e., $q_{i-1,i}$, and the expected number of transmissions under the failure of the initial transmission, i.e., $\frac{1}{p_{i,i}}$. Therefore, the equation simply implies that a low cETX value is achievable where there are two conditions: (i) a small chance of the failure in the initial transmission, and (ii) a high chance of recovering from the failure in case the initial transmission fails.

Special Case: Eq.(2) shows that cETX is a function of spatiotemporal ($q_{i-1,i}$) and temporal ($p_{i,i}$) correlation parameters. However, the initial link e_1 is a special case as

there is no link preceding it. In other words, e_1 has no link to be spatiotemporally correlated to it. Therefore $q_{0,1}$ is expressed sorely in terms of temporal correlation parameters, $p_{1,1}$ and $q_{1,1}$, to be the steady state probability of F_1. Please note that $q_{1,1}$ is found in the original Gilbert Model (q in Figure 7). Borrowing the steady state probability in Eq.(1) and rewriting with our notations, we have

$$q_{0,1} = \frac{q_{1,1}}{p_{1,1} + q_{1,1}} \tag{3}$$

The rationale behind this equation is as follows. The first transmission on the initial link is triggered at an arbitrary time instant, whenever the sender has a packet to transmit. This indicates that we need to estimate the link state at time t_n without the knowledge of the state at t_{n-1}. In this case, our best estimate becomes the steady state probability of S_1, which is simply the ratio of the time e_1 spent in S_1. Now, we can finally obtain $cETX_{e_1}$ by plugging in Eq.(3) to Eq.(2).

$$cETX_{e_1} = 1 + \frac{q_{1,1}}{(p_{1,1} + q_{1,1}) \cdot p_{1,1}} \tag{4}$$

Path cETX: Our metric retains the additive property of ETX, indicating that path cETX is the sum of link cETXs in the path. This serves as the key that allows us to find the optimal path with cETX with appropriate modifications to traditional shortest path algorithms, which will be discussed in later part of the paper. For a proof on the additive property, let us again consider the network and its model in Figures 10 and 11, where $cETX_E$ represents the cETX of the entire N-hop path. Then, $cETX_E$ is the expected first passage time from state I to S_N. Let the first passage time from state I to S_1 be denoted by a random variable Y_1, from S_1 to S_2 as Y_2, and so on until Y_N. Then, by definition $cETX_E$ is the expected value of the sum of all Y_i, i.e., $cETX_E = E[\Sigma_{i=1}^{N} Y_i]$. Due to the linearity of expectation and since $cETX_{e_i} = E[Y_i]$, we have

$$cETX_E = \sum_{i=1}^{n} cETX_{e_i} \tag{5}$$

Hence the additive property holds. We also note that cETX is indeed a generalized version of ETX, and it simply reduces to ETX under independent packet receptions. Proof on the relationship between cETX and ETX under different degrees of correlations is given in Appendix A.

V. Implementation Issues

This section describes obtaining the parameters (i.e., p and q) needed to compute cETX online, where we introduce *burst probing* to enable precise measuring of the true performances in wireless links.

A. Parameter Computation

Among the parameters required by our design, those related to temporal correlation within a link are p and q. We again use S_n and F_n to denote the transmission success and failure at t_n. Let us compute the p and q values for e_2 in Figure 12. Maximum likely estimation for these parameters can be obtained simply by counting the number of transitions between success and failure, which turns out to be $p_{2,2} = Pr(S_2^n | F_2^{n-1}) = 1/3$ and $q_{2,2} = Pr(F_2^n | S_2^{n-1}) = 1/5$ for $0 < n \leq 11$. Similarly, the spatiotemporal correlation parameter when e_1 precedes e_2 is also computed as $q_{1,2} = Pr(F_2^n | S_1^{n-1}) = 1/2$.

e_1	F	F	S	F	S	F	F	S	S	F	F	S
e_2	F	F	F	F	S	F	F	S	S	S	S	S
	t_0	t_1	t_2	t_3	t_4	t_5	t_6	t_7	t_8	t_9	t_{10}	t_{11}

Fig. 12. Parameter Computation Example.

B. Measurement in Practice

Probing refers to the technique of transmitting a small number of packets to support some fundamental functions including link quality measurement and neighbor discovery. Thus probes are commonly utilized in various state-of-the-art link metrics [11], [15], [30], [31]. Specifically, they adopt the classical periodic probing, where a single probe message is broadcast every fixed interval. However this mechanism suffers from limitations in measuring link performances; We observe that immediate retransmissions and relays induce a stream of packets within a short time interval to impose correlations between transmissions, which cannot be captured by periodic probes. To address this issue, we propose burst probing, where a batch of consecutive probes are sent at a short time interval. In the meantime, to keep the overhead at a reasonable level, the interval between probe bursts is set such that the number of probe packets per unit time is kept the same as that of periodic probing. This ensures the equivalent amount of overhead when cETX replaces ETX.

Unlike temporal parameters, measuring the spatiotemporal parameter via probing incurs additional overhead. This is because the spatiotemporal parameter for a link needs to be measured for every preceding link. To avoid such overhead, we obtain spatiotemporal parameters via the normal data traffic. Recall that the spatiotemporal correlation parameter is simply the failing probability of the initial transmission, just after the packet is received from the preceding link. This statistic can be easily collected; whenever a node receives a data packet, it records the preceding link, as well as the transmission success/failure of the initial transmission. This information is piggybacked on probes to be broadcast to its neighbors. To sum up, cETX assumes spatiotemporal independence under data traffic volume insufficient to obtain spatiotemporal parameter, where the accuracy of cETX nevertheless exceeds that of ETX due to the consideration of temporal correlation. Spatiotemporal correlation is reflected as the traffic increases, where multiple data flows in the network offer cETX with more opportunity to select better routes considering spatiotemporal correlation.

C. Overhead Under Link Dynamics

We run an experiment to compare the link estimation performances of cETX and ETX in relation to the overhead they induce. To summarize, our result indicates estimation error for cETX is only 1/3 of ETX, at the cost of only 0.7% additional overhead. Experimental details are as follows: Burst probing in cETX occurs every 40s, where five consecutive

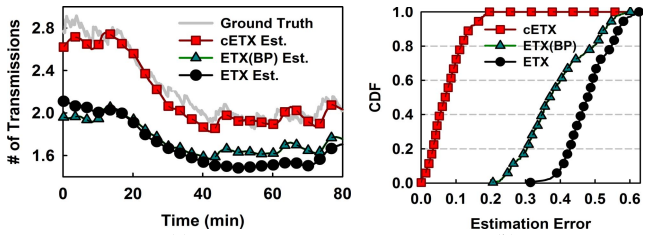

Fig. 13. Link estimation with cETX closely reflects the actual value (i.e., the ground truth) while ETX is rather optimistic. This is because cETX accounts for bursty losses which ETX fails to capture. (a) Estimation under dynamics. (b) Error distribution.

probes are sent each time. Conversely, ETX periodically (as per the original literature [12]) sends one probe every 8s. We note that both cETX and ETX induce the consistent overhead of 1/8 probe per second, indicating a fair comparison (i.e., under the same overhead). To further maintain fairness, both metrics use the history of up to 90 probes, following the value suggested by ETX [12]. In other words, when there is a data packet to be forwarded (every 10s in our case), both metrics use the history of the last 90 probes to estimate the number of (re)transmissions until a successful delivery. Then, the estimations are compared to the number of transmissions that actually occurs, to verify their accuracies. The 80-minute experiment consists of 11 MICAz nodes, v_1 through v_{11}. One node (v_1) serves as the sender while all others are receivers.

Figure 13(a) shows the result on a link between v_1 and v_8. The ground truth indicates the actual number of transmissions, while other curves are estimations based on probe history. Furthermore, Figure 13(b) exhibits the distribution of the estimation error (i.e., the absolute difference from the ground truth). We note that there are two versions of ETX in the figure, where one is the original ETX with periodic probing and the other is the modified ETX with burst probing. From the figures, we find that the estimate of cETX is far better than both versions of ETX. The average estimation error of cETX, ETX with burst probing, and original ETX in all ten links are 0.16, 0.42, and 0.48. The performance of ETX with burst probing sits in between cETX and the original ETX because it benefits from burst probing which mimics the data (re)transmission scenario, but it fails to accurately capture the correlation within. We note that the degree of cETX's advantage in accuracy applies to the link metrics built on top of ETX, such as 4B [15].

The overhead incurred by probes is approximately 3.2% of the total energy consumed. Since probing is adopted in the majority of the link metrics, its overhead should be amortized. On the other hand, exclusive overhead introduced by our design is the extra information piggybacked on probe packets. This takes up a tiny portion of about 0.7% of the total energy consumption.

VI. Unicast/Broadcast Over cETX

By simply replacing the popular metric of ETX, cETX can be generically applied to many protocols. This section presents how optimality is maintained in unicast protocols, followed by the benefit to broadcast schemes.

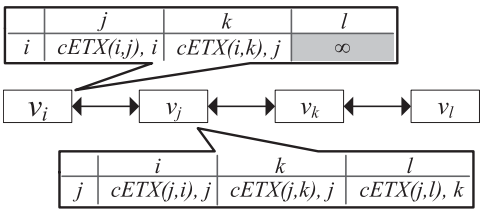

Fig. 14. cETX in Unicast – Example Scenario.

A. Application to Unicast

When spatiotemporal correlation is considered, the cETX value of a link is dependent on the preceding link. This is not considered in traditional routing algorithms and hence direct application of such schemes yields sub-optimal path selection. We propose both distributed and centralized algorithm for optimal shortest path selection, where, for brevity, the discussion on the latter is deferred to Appendix B. In the following we demonstrate via an example, how optimal shortest path can be found in a distributed manner using distance vector with two-hop information.

Let us consider a simple four-node network in Figure 14, where $cETX(i,j)$ indicates cETX from node v_i to v_j. Initially, nodes attain local information about their two-hop neighbors by exchanging information between one-hop neighbors. Then the problem becomes: How cETX beyond two hops can be obtained through further iterative exchanges. That is, how the gray box in v_i's distance vector (i.e., $cETX(i,l)$) can be found. First, we note that $cETX(i,l) \neq cETX(i,j) + cETX(j,l)$, as $cETX(j,l)$ does not reflect the effect of correlation among the link between v_i and v_j and the link between v_j and v_k. Instead, $cETX(i,l)$ can be obtained via the below relationship:

$$cETX(i,l) = cETX(i,k) + cETX(j,l) - cETX(j,k)$$

where last the term, $cETX(j,k)$, is the cost of link between v_j and v_k *not considering* the correlation with the link between v_i and v_j (i.e., the special case in Section IV-D). Referring back to Figure 14, the above equation implies that v_i can obtain $cETX(i,l)$ via exchange of distance vector with its direct neighbor, v_j. In fact, the equation can be generally applied to finding cETX to any multiple hops (i.e., v_l of any hop distance from v_i), given that v_j and v_k are one and two-hop neighbors to v_i.

The Case of Convergecast: Support of unicast, the most fundamental data delivery mechanism, indicates cETX's applicability to a wide range of protocols whom unicast serves as their basis operation. Convergecast [47] is one example – packets from multiple sources are delivered over unicast to a single destination, the sink. In convergecast the impact of spatiotemporal correlation is determined by immediate or delayed forwarding (in case of aggregation [8]), where cETX inherently covers both the cases via its unicast support.

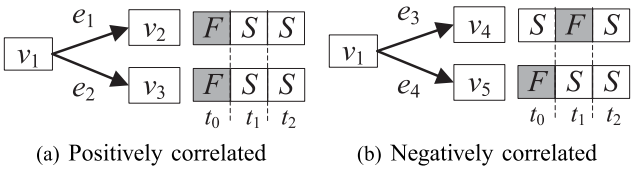

(a) Positively correlated (b) Negatively correlated

Fig. 15. Benefit of cETX in broadcast: (a) and (b) require 1.25 and 1.66 transmissions to deliver 2 packets to both receivers. Performance improves when receivers are positively correlated, which can be captured by cETX.

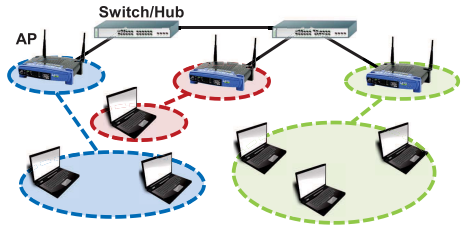

Fig. 16. Collaborative broadcast in Wi-Fi. APs connected via wires cooperatively deliver data to all the users (laptops). Dotted circles indicate user groups assigned to APs. In cETX a group consists of highly correlated users.

B. Application to Broadcast

This section presents how cETX can help improve the performances of broadcast protocols. First, let's consider the positively correlated case in Figure 15(a). If v_1 starts broadcast at t_0, the two receivers will both receive the second packet at t_1, causing two transmissions to deliver the packet to both receivers. If the broadcast starts at t_1, the two receivers immediately receive the packet, indicating that a single transmission is consumed. Similarly, at t_2, only one transmission is required. Therefore, an average of $(2+1+1)/3 = 1.25$ transmissions are needed for the network in Figure 15(a), while it is $(2+2+1)/3 = 1.66$ in Figure 15(b). Here we calculate the expected number of transmissions – $E(T)$ for a source node to reliably broadcast one packet to all the receivers with the consideration of temporal and spatial correlation using cETX. Without loss of generality, we assume that the link quality of the N receivers satisfies $Pr(S_1^n) \geq Pr(S_2^n) \geq \ldots \geq Pr(S_N^n)$. Since the node with a better link receives most of the packets earlier than the node with a worse link [43], we have

$$\begin{aligned} E(T) &= 1 + \frac{q_{1,1}}{(p_{1,1}+q_{1,1})\cdot p_{1,1}} + \sum_{i=2}^{N} \frac{q_{i-1,i}}{p_{i,i}} \\ &= cETX_{e_1} + \sum_{i=2}^{N} (cETX_{e_i} - 1) \\ &= \sum_{i=1}^{N} cETX_{e_i} - N + 1 \end{aligned} \tag{6}$$

This lets cETX to be integrated within various broadcast protocols by selecting forwarder which minimizes $E(T)$.

Eq. (6) can be further applied to a novel communication paradigm for Wi-Fi networks, demonstrated in Figure 16. In collaborative broadcast multiple APs connected via wires share the same data to collaboratively deliver it to all users. Grouping and assigning users to APs are done via Eq.(6). Both ordinary and collaborative broadcasts are further described and evaluated in the next section.

(a)

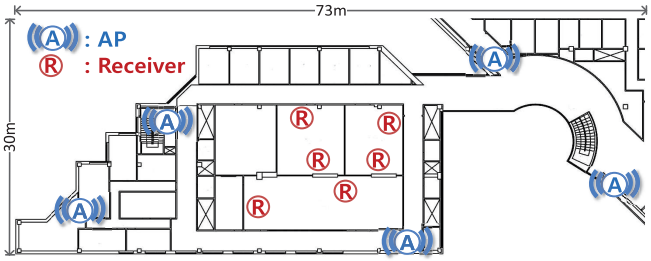

(b)

Fig. 17. ZigBee and Wi-Fi Testbeds. (a) ZigBee (lab). (b) Wi-Fi (university building).

VII. Testbed Experimentation

Though this section we demonstrate the universal applicability of our design to various wireless technologies, operating under different scenarios and environments: cETX is evaluated on ZigBee (802.15.4) and Wi-Fi (802.11) testbeds, under unicast and broadcast running twelve protocols.

A. Baseline

Various representative studies in unicast and broadcast domains are implemented for cETX evaluation.

• **Unicast**: We adopt cETX in three representative unicast routing protocols. **(i) LQSR** [14]: Extends the DSR [22] protocol by taking unreliable links into account. **(ii) srcRR** [4]: Similar to LQSR, but without path switching to improve network robustness. **(iii) OLSR** [19]: Routing is executed only through a subset of nodes (i.e, Multi Point Relays) to reduce the control overhead. The three protocols offer different degrees of freedom in path selection to affect the benefit of cETX.

• **Broadcast**: We integrate cETX to nine classical broadcast protocols with diverse underlying network structures, showing the wide applicability of cETX. **(i) tree based**: C-Tree [7], **(ii) cluster based**: forwarding node cluster (Cluster) [48], **(iii) Multi-Point Relay**: MPR [35], **(iv) pruning based**: Self Pruning (SP [29]), Dominating Pruning (DP [29]), Partial Dominating Pruning (PDP [32]), and Total Dominating Pruning (TDP [32]), **(v) RNG based**: RNG relay subset (RNG [20]), and finally, **(vi) network coding [23] based broadcast protocols**: CODEB [28].

B. Performance Metrics

The following metrics are adopted throughout evaluation.

• **Number of Transmissions**: The average number of (re)transmissions to deliver one packet to the destination. Less number of transmissions indicate energy savings.

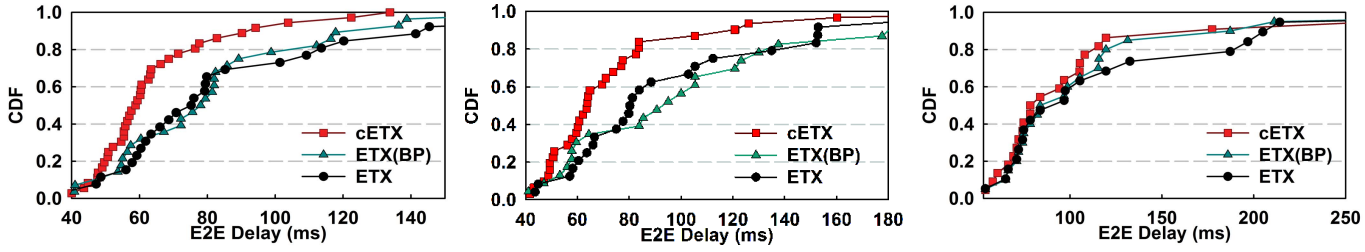

Fig. 18. End-to-End Delay: cETX reduces the delay from 10.7% to 26.7% compared to ETX, where the improvement is achieved by the wiser route selection. LQSR allows the highest degree of freedom in the path selection, thus benefits most from cETX. (a) LQSR. (b) srcRR. (c) OLSR.

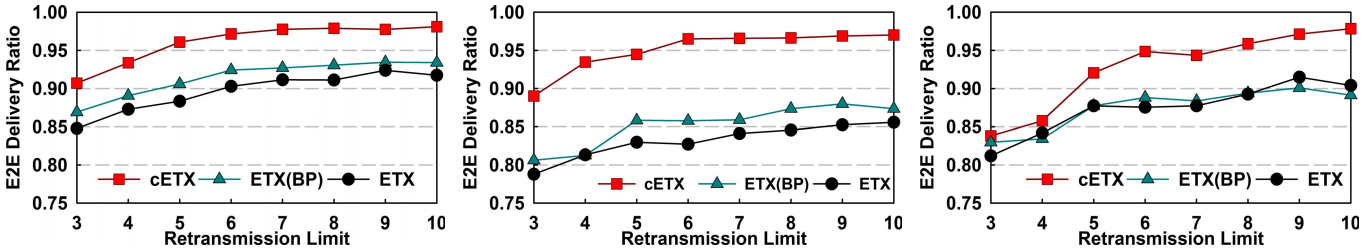

Fig. 19. End-to-End Delivery Ratio: cETX tends to select links without burst failures, that are safer from exceeding the retransmission limit. This naturally leads to a higher delivery ratio compared to ETX. (a) LQSR. (b) srcRR. (c) OLSR.

• **End-to-End Delivery Delay**: The average latency for a packet to be delivered to the destination.

• **End-to-End Delivery Ratio**: The success probability of a packet delivered end-to-end. That is, the number of (re)transmissions in each link in a path do not exceed the retransmission limit.

C. Experiment Setup

Experimental results in this section are obtained from two physical testbeds, ZigBee and Wi-Fi, with below settings.

• **ZigBee**: We randomly deploy 22 MICAz motes running TinyOS as shown in Figure 17(a). Transmission power is set to be -25dBm to ensure multi-hop network, up to 5 hops. Node placement is kept the same for all evaluated metrics for fairness. Experiment for each metric lasts for two hours, during which an end-to-end packet delivery is made every four seconds, for a total of 1,800 deliveries per metric. CSMA is performed for each (re)transmission with random delay, where the average interval between retransmissions is approximately $6ms$. We limit the maximum number of retransmissions for each packet to be 7 (unless otherwise stated) following most practical systems to safeguard networks from being overwhelmed by retransmissions and collisions. Lastly, time stamps and sequence numbers of the delivered packets are logged in the nodes' flash, and uploaded to a PC at the end of the experiment.

• **Wi-Fi**: Depicted in Figure 17(b), five APs are installed in the corners of the floor, where we use laptops with the `Lorcon2` packet injection library [2] to play the role of AP generating downstream traffic. It is a reasonable approach since laptops/PCs are frequently used as APs in practice via software AP [1]. Six receivers are placed in three different rooms, separated by concrete walls. Although mainly 802.11g on channel 6 is used for its popularity, analyses later in the section implies a similar benefit in 802.11b and 802.11n as well. A total of 10^5 packet transmissions are made in 40 minutes, with the power of 20dBm. Links with packet reception ratios from 10% to 95% are observed, where we commonly apply EWMA (Exponential Weighted Moving Average) on every metric. Control overhead of different probing (i.e., burst probing in cETX and ETX(BP), and periodic probing in ETX) is kept consistent for fairness.

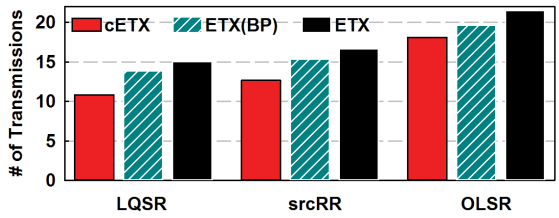

Fig. 20. cETX saves 27.8%, 24.1%, and 15.8% of transmissions for LQSR, srcRR, and OLSR, compared to ETX.

D. Unicast

Figure 20 depicts the performance of cETX on unicast, obtained from the ZigBee testbed in Figure 17(a). Compared to ETX, cETX saves 27.8%, 24.1%, and 15.8% of transmissions for LQSR, srcRR, and OLSR. This demonstrates that cETX makes wiser routing decisions than ETX. Compared to ETX(BP), the percentage of savings becomes 21.6%, 17.5%, and 7.7%. This is because ETX(BP) benefits from burst probing for a slight performance enhancement over the original ETX. Furthermore, the advantage of cETX is the largest for LQSR and smallest for OLSR. The reason for this lies in the number of paths to choose from. While LQSR grants the most freedom in selecting paths, srcRR and OLSR restrict the frequent path switch to avoid high control overhead. Especially, OLSR only allows paths with MPR (Multi Point Relay) nodes. Figure 18 shows the end-to-end delay of metrics in the three protocols. cETX again

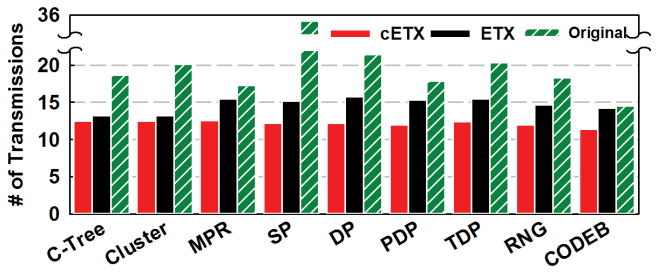

Fig. 21. The Performance in Broadcast: cETX saves an average of 37% transmissions in nine broadcast protocols.

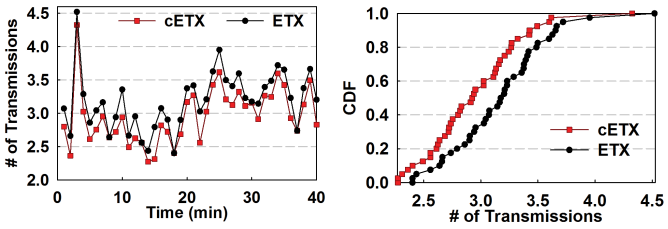

(a) (b)

Fig. 22. In (a) cETX consistently reduces number of broadcasts compared to ETX, indicating energy savings. This is shown as distribution in (b).

exhibits the best performance, where the average reduction in delay ranged from 10.7% to 26.7%. Again LQSR obtains the biggest performance improvement due to the largest selection of paths.

• **Impact of Retransmission Limit:** Now we vary the limitation in the number of retransmissions 3-10 and investigate its effect on the performance. Packet in delivery is dropped whenever the number of transmissions in a single link exceeds the limit, indicating failure in the end-to-end delivery. Note that exceeding the limit requires a link exhibiting continuous failures, which cETX precisely avoids to select. On the other hand, ETX blindly selects paths without considering this issue, leading to a worse delivery ratio. As shown in Figure 19, regardless of protocol cETX consistently achieves delivery ratios of over 94% for retransmission limit of 7 or higher.

E. Broadcast

The experimental results on nine classical reliable broadcast protocols, tested on ZigBee testbed, are shown in Figure 21. On average, the protocols need 20.5 transmissions to guarantee delivery of a packet to the entire network, while the number becomes 14.7 and 12.2 for ETX and cETX. Knowing that CODEB saves 31.6% of transmissions compared to the schemes without network coding, our design makes a further 21.4% improvement upon CODEB due to following reasons: a low link correlation may cause the nodes in a cluster to lose different packets, causing more retransmissions. With the consideration on spatial and temporal correlations, the protocols benefit from cETX to select forwarders with the minimum transmission cost (i.e., $min(\frac{E(T)}{N})$), thus forming clusters with high correlations.

Figure 22 shows the improvement achieved for collaborative broadcast on Wi-Fi testbed depicted in Figure 17(b). Five APs collaboratively deliver 10^5 packets to all six receivers. As cETX allows grouping highly correlated receivers to minimize retransmissions, its transmission cost is consistently less than or equal to that of ETX. The reduction is as large as 34.1%.

F. Performance Insights

This section provides analysis on *why* cETX performs better than ETX. Results on ZigBee platform are obtained from the 11-node experiment in Section V-C. For Wi-Fi, experiments with six receivers and 2×10^5 packets are analyzed for each 802.11 variant: b, g, and n. We also analyze large-scale public Wi-Fi traces (5.6×10^5 packets from 560 links) from the MIT's Roofnet project [3] to validate the generality of our design.

•**Interpretation accuracy in unicast:** We first show the metrics' abilities to accurately interpret the probe reception history. That is, given the history, we observe how precisely a metric captures the performance of the corresponding link. This is done by comparing ETX and cETX values to the true value, introduced in Section II-B. We use *error* as the measure of interpretation quality, which is the absolute difference between the metric and the true value. The result on ZigBee platform is depicted in Figure 23(a). Error for cETX is less than that of ETX for most of the time, where it is 70.2% less on average. This is because ETX fails to capture highly correlated burst failures. This trend continues to Wi-Fi in Figure 23(b) regardless of its variants; ETX errors exceed those of cETX by 45.1%, 84.7%, and 160.3% in 802.11b, g, and n. Analysis on the Roofnet trace, which is a mixture of 802.11b and g, indicate the error is 49.6% larger in ETX. We note that error in Roofnet trace is generally smaller compared to our experiments; Roofnet is measured in outdoor deployment, where the degree of interference (i.e., the main cause of burst failures) is limited.

•**Interpretation accuracy in broadcast:** In both traditional and collaborative broadcasts, multiple receivers form a cluster in which members receive the packets from the designated sender. (i.e., APs) A smart grouping of receivers and assigning them with the right sender play a key role in determining the efficiency of the network. With the consideration of link correlation, cETX shows an improved accuracy compared to ETX in computing the expected number of transmissions required for a cluster for a given sender, as presented in Figure 23(c). Similarly to the unicast case, error is defined to be the absolute value of the difference of the true value and the values computed by cETX and ETX. The figure shows adopting cETX reduces the error by up to 67.6% in Wi-Fi where in ZigBee it is as high as 91.4%. This is because multiple low-power ZigBee links can easily be victims of cross-network interferences, inducing correlation among links. On average, cETX reduces the error by 21.5% and 75.3% in Wi-Fi and ZigBee, respectively. This advantage provides a rational explanation of the transmission (i.e., energy) saving achieved in the broadcast protocols shown earlier in the section.

•**Estimation accuracy and route selection:** An inaccurate interpretation leads to an imprecise link quality estimation and further, a sub-optimal route selection. We show how

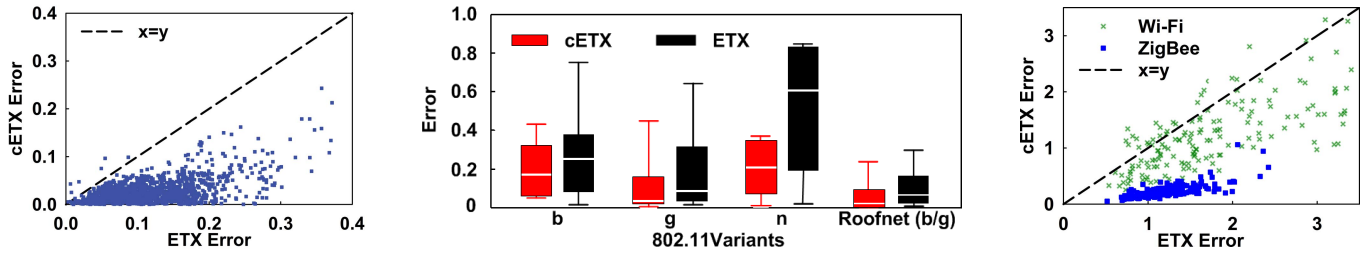

(a) (b) (c)

Fig. 23. Interpretation error is notably lower in cETX. In unicast cETX error is less than half of ETX. The performance of ETX rapidly drops in 802.11n where the fast transmission rate induces a high temporal correlation among consecutive transmissions. Roofnet shows the smallest error due to the outdoor environment with low degree of wireless interference. Under broadcast cETX reduces the error by 72.3% and 21.5% on ZigBee and Wi-Fi, respectively. (a) Unicast (ZigBee). (b) Unicast (Wi-Fi). (c) Broadcast.

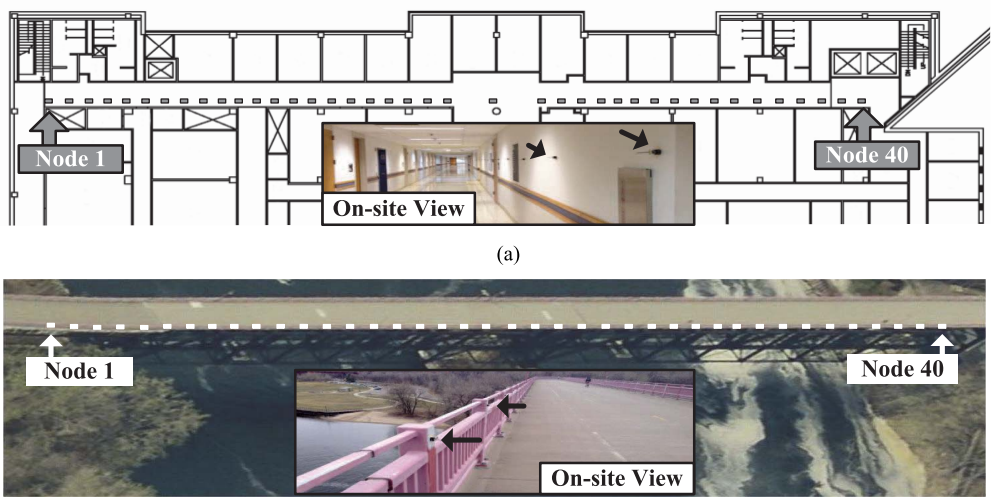

(a)

(b)

Fig. 24. Indoor (corridor) and outdoor (bridge) experiment setup. On each site 40 MICAz nodes are linearly deployed every $1.8m$, for $70m$. In the corridor nodes were attached to the wall, $1.8m$ above the floor, while on the bridge they were deployed on the steel fence of height $1.5m$. The corridor is within a university building with heavy Wi-Fi traffic. (a) Corridor. (b) Bridge.

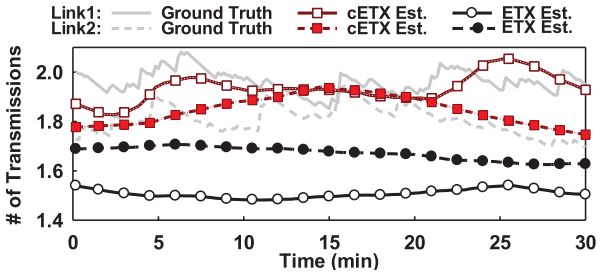

Fig. 25. Unlike ETX, cETX accurately estimates the ground truth, where the quality of Link2 is either better or at least similar to that of Link1.

this occurs in practice via Figure 25, showing the estimated and real number of transmissions on two distinct links for 30 minutes. The figure conveys two ideas: (i) cETX estimation is more precise and thus (ii) cETX makes better routing decision. When making a selection between links 1 and 2, ETX suggests link 1 should be chosen over link 2, due to the lower ETX value. However, the ground truth indicates otherwise, i.e., link 2 always has a better or similar (at 17^{th} min) performance than link 1. cETX is free from this problem, explaining the performance gain obtained in the unicast and broadcast algorithms in the earlier parts of the section.

VIII. In-Situ Deployment

To further demonstrate the feasibility of cETX in real-world applications, we conduct experiments under practical indoor and outdoor settings. Forty MICAz nodes are deployed in a corridor in a university building and on a bridge crossing a river – common sites for popular applications including tracking and maintenance/safety monitoring – as shown in Figure 24. Nodes are deployed every $1.8m$ spanning $70m$ end to end. The transmission power is set to be -15dBm to assure multiple neighbors, where each node roughly has 10-12 neighbors (i.e, 5-6 neighbors to the node's right and left). Other parameters are kept the same as previous experiments. A thousand end-to-end (i.e., from node 1 to 40) packet deliveries are made, via LQSR embedding either ETX or cETX.

Results on delivery delay, shown in Figure 26(a), suggests that cETX's performance gain is more significant in the corridor (21.5% reduction) than on the bridge (8.9% reduction). This is due to the degree of wireless interference; In the university building hundreds of Wi-Fi users are connected to over fifty Wi-Fi access points, creating excessive amount of wireless interference (up to 60%). Conversely, the closest building to the bridge was more than 50 feet away, inducing significantly less intereference (less than 10%). The bursty

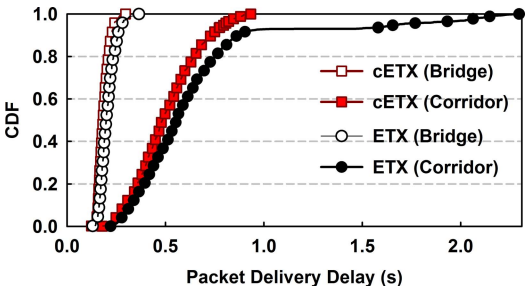

(a)

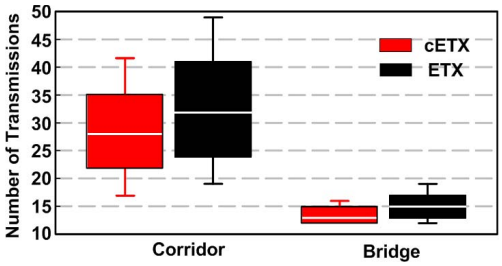

(b)

Fig. 26. In-situ results for 10^3 packet deliveries. (a) Delay distribution. (b) Number of transmissions.

nature of interference causes burst failures in the experiment, forcing ETX to select poorly performing paths suffering from long delivery delays well above 1 second. Similar observation can be made in Figure 26(b). The average number of transmissions are 28.8 and 36.9 for cETX and ETX in the corridor, respectively, indicating 21.9% reduction. Due to the same reason as in the delay case, smaller degree of reduction (9%) is observed on the bridge, compared to what is achieved in the corridor. This effecitvely demonstrates the increasing benefit of cETX under practical inteference volumn and pattern.

IX. Related Work

Our work is built on top of two phenomena studied separately – temporal and spatiotemporal correlation. We summarize how they have been studied in relation to our work.

• **Temporal Correlation:** The impact of temporal correlation in ZigBee network, as well as in Wi-Fi, has been demonstrated clearly via extensive measurements and analyses in [39], where the authors propose a metric to quantify the degree of correlation. Furthermore, the works including BRE [6], 4C [30], and TALENT [31] exploit short-term dynamics based on packet overhearing to utilize intermittent and burst links. In RNP [11] and mETX [27], temporal properties of links were considered in routing, by counting consecutive failures and taking the variance of failure probability, respectively. However, the works in this category pays little or no attention to correlation across different links.

• **Spatial Correlation:** The comprehensive study on packet-level spatial correlation in [38] suggests a metric to predict performances of diversity-based protocols based on the intensity of correlation. To date, the phenomenon has been exploited in a wide range of wireless domains including ZigBee [53], Wi-Fi [38], and cellular networks [31]. For instance, it was utilized to improve the performances of network coding [24], [44], broadcast [5], [18], and opportunistic routing [26], [42]. Furthermore, Spatial correlation was studied in the presence of constructive interference to achieve fast data dissemination [13]. In this work we consider spatiotemporal correlation, which expands the effect of spatial correlation to the time domain. The unified design allows us to improve unicast and broadcast performance. In addition, the previous studies focus on particular protocol designs, while this work provides a generalized form of the widely-adopted ETX. Our work can broadly improve a wide range of protocols.

X. Conclusion

Our empirical study reveals the spatiotemporal correlations among wireless links, to shed light on the possibility of further improvement in network performance; The most widely adopted link metric, ETX, fails to reflect the true link performance due to the ignorance of correlations. We propose cETX to compensate for the inaccuracy – a generalized version of ETX capturing not only temporal correlation but also spatiotemporal correlation. As our design keeps the intuitive idea of ETX intact, cETX simply replaces ETX in a wide range of existing protocols to improve their performance. Our evaluations on both ZigBee and Wi-Fi testbeds demonstrate that cETX cuts down the metric error by 75.8% and 62.1%, and saves 22% and 37% communication cost for 3 unicast and 9 broadcast protocols with only 0.7% additional overhead.

Appendix A
The Properties of cETX

In this appendix we provide the relationship between cETX and ETX, under various degrees of correlations.

• **Under independence:** cETX is a generalized version of ETX, where cETX simply reduces to ETX when packet receptions are independent. For simplicity, we omit the subscript for the following parts of the section. For an arbitrary link, spatiotemporal independence turns $cETX$ from Eq.(2) to the form of Eq.(4). Then, when transmissions are temporally independent,

$$Pr(S^n|F^{n-1}) = Pr(S^n|S^{n-1})$$

which leads to $p+q=1$. By plugging in this condition within Eq.(4), we have

$$cETX = \frac{p+q}{p} = \frac{1}{Pr(S^n)} = ETX$$

where we used Eq.(3) and the rationale behind it. Thus, cETX is equivalent to ETX when transmissions are independent.

• **Effect of temporal correlation:** Here we show how cETX is determined in relation to correlations. For clarity, in direct comparison to ETX, we use cETX in Eq.(4). When link faces failure burst due to temporal correlation, the following condition holds:

$$Pr(F^n|F^{n-1}) > Pr(F^n|S^{n-1})$$

We thus have $p+q<1$. Plugging in the condition within Eq.(4), we obtain

$$cETX = \frac{q}{(p+q)\cdot p} + 1 > \frac{q}{p} + 1 = ETX$$

Therefore, cETX is larger than ETX upon bursty failure. In other words, ETX normally underestimates the transmission cost because of the ignorance of temporal correlation.

- **Effect of spatiotemporal correlation:** Conversely to temporal correlation, the spatiotemporal correlation enforces to ETX to overestimate the transmission cost of a link, leading to a bigger value compared to cETX. When link e_i is preceded by e_{i-1}, spatiotemporal correlation offers a lower chance of packet forwarding failure on e_i immediately after the packet has passed the previous link, e_{i-1}. This yields

$$Pr(F_i^n|S_{i-1}^{n-1}) = q_{i-1,i} < \frac{q_{i,i}}{p_{i,i}+q_{i,i}} = Pr(F_i^n)$$

To isolate the impact of spatiotemporal correlation, let us assume that there is no temporal correlation within e_i, or in other words, $p_{i,i}+q_{i,i} = 1$. Plugging this in the above equation yields $q_{i-1,i} < q_{i,i}$. From this condition, we have

$$cETX = 1 + \frac{q_{i-1,i}}{p_{i,i}} < 1 + \frac{q_{i,i}}{p_{i,i}} = ETX$$

indicating ETX yields cost overestimation, by ignoring the effect the spatiotemporal correlation between consecutive links.

APPENDIX B
CENTRALIZED ROUTING OVER CETX

Algorithm 1 Correlation-Aware Floyd Warshall

Input: $w[1...N, 1...N, 1...N]$, where $w[i,j,k]$ indicates link cETX from node i to j, given the preceding link is from node k to i

Output: $d[1..N, 1...N]$ and $pred[1..N, 1...N]$, where d indicates cETX of minimum cost path between node pairs, and $pred$ is the matrix of predecessor pointers

1: **for** $\forall$ node pairs i, j there $\exists$ direct path from i to j **do**
2: $d[i,j] \Leftarrow w[i,j,i]$, $prev[i,j] \Leftarrow i, next[i,j] \Leftarrow j$
3: **end for**
4: **for** k, i, j = 1 to n **do**
5: $adj \Leftarrow w[k, next[k,j], prev[i,k]] - w[k, next[k,j], k]$
6: **if** $d[i,k] + d[k,j] + adj < d[i,j]$ **then**
7: $d[i,j] \Leftarrow d[i,k] + d[k,j] + adj$
8: $prev[i,j] \Leftarrow prev[k,j], next[i,j] \Leftarrow next[i,k]$
9: $pred[i,j] \Leftarrow k$
10: **end if**
11: **end for**

To find the optimal minimum-cost path when links are spatiotemporally correlated, we take the dynamic programming approach by modifying the *Floyd-Warshall* all pairs shortest paths algorithm. The pseudo code is shown in Algorithm 1. Our algorithm follows the main idea of the original version – whenever the path cost from v_i to v_j can be lowered by passing through v_k, the path is newly set to be the concatenation of the path from v_i to v_k followed by the path from v_k to v_j. However, the difference comes when we compute the cost of the concatenated path. The cETX value of the new path does not equal the sum of the cETX values in two paths. This is because the cETX value of the first link in the latter path is spatiotemporally affected by the last link in the former path. This issue can be addressed simply by adjusting the cETX value of the affected link to reflect the correlation.

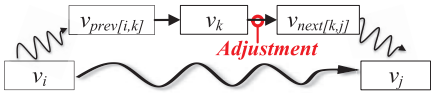

Fig. 27. In setting the path between v_i and v_j to be the concatenation of the two subpaths $v_i \rightarrow ... \rightarrow v_k$ and $v_k \rightarrow ... \rightarrow v_j$, spatiotemporal correlation is considered by adjusting cETX of the marked link before subpath cETX can be summed to represent the distance of the path.

Let $w[i,j,k]$ indicate the cETX value of the link from v_i to v_j while v_k is preceding v_j. Furthermore, in a path from v_i to v_j, let $v_{prev[i,j]}$ and $v_{next[i,j]}$ to be the node preceding v_j and the node following v_i, respectively. Then, when two paths, i.e., v_i to v_k and v_k to v_j, are concatenated, we adjust the cETX value of the link from v_k to $v_{next[k,j]}$ to be $w[k, next[k,j], prev[i,k]]$. This scenario is presented in Figure 27, where the computation detail is shown in lines 6 and 8 in Algorithm 1. We note that the computational complexity is kept the same (i.e., $O(n^3)$) as the original Floyd-Warshall.

REFERENCES

[1] *Hostapd*. Accessed on Apr. 10, 2015. [Online]. Available: http://hostap.epitest.fi/hostapd/
[2] *Lorcon Wireless Packet Injection Lib*. Accessed on Apr. 10, 2015. [Online]. Available: https://code.google.com/p/lorcon/
[3] *Mit Roofnet*. Accessed on Apr. 10, 2015. [Online]. Available: http://pdos.csail.mit.edu/roofnet/doku.php?id=publications#sigcomm_trac%es/
[4] D. Aguayo, J. Bicket, and R. Morris, "Srcrr: A high throughput routing protocol for 802.11 mesh networks," Ph.D. dissertation, Dept. Elect. Eng. Comput. Sci., MIT, Cambridge, MA, USA, 2004.
[5] S. M. I. Alam, S. Sultana, Y. C. Hu, and S. Fahmy, "Link correlation and network coding in broadcast protocols for wireless sensor networks," in *Proc. SECON*, 2012, pp. 1–6.
[6] M. H. Alizai, O. Landsiedel, J. A. B. Link, S. Götz, and K. Wehrle, "Bursty traffic over bursty links," in *Proc. SenSys*, 2009, pp. 1–14.
[7] K. Alzoubi, P. Wan, and O. Frieder, "New distributed algorithm for connected dominating set in wireless ad hoc networks," in *Proc. Hawaii Int. Conf. Syst. Sci.*, 2002, pp. 3849–3855.
[8] M. Bagaa, M. Younis, D. Djenouri, A. Derhab, and N. Badache, "Distributed low-latency data aggregation scheduling in wireless sensor networks," *ACM Trans. Sensor Netw.*, vol. 11, no. 3, pp. 49:1–49:36, 2015.
[9] R. Banirazi, E. A. Jonckheere, and B. Krishnamachari, "Heat-diffusion: Pareto optimal dynamic routing for time-varying wireless networks," in *Proc. INFOCOM*, 2014, pp. 325–333.
[10] M. Buettner, G. V. Yee, E. Anderson, and R. Han, "X-MAC: A short preamble MAC protocol for duty-cycled wireless sensor networks," in *Proc. SenSys*, 2006, pp. 1–18.
[11] A. Cerpa, J. L. Wong, M. Potkonjak, and D. Estrin, "Temporal properties of low power wireless links: Modeling and implications on multi-hop routing," in *Proc. MobiHoc*, 2005, pp. 414–425.
[12] D. S. J. De Couto, D. Aguayo, J. Bicket, and R. Morris, "A high-throughput path metric for multi-hop wireless routing," in *Proc. MobiCom*, 2003, pp. 419–434.
[13] M. Doddavenkatappa, M. C. Chan, and B. Leong, "Splash: Fast data dissemination with constructive interference in wireless sensor networks," in *Proc. NSDI*, 2013, pp. 269–282.
[14] R. Draves, J. Padhye, and B. Zill, "Routing in multi-radio, multi-hop wireless mesh networks," in *Proc. MobiCom*, 2004, pp. 114–128.
[15] R. Fonseca, O. Gnawali, K. Jamieson, and P. Levis, "Four-bit wireless link estimation," in *Proc. HotNets*, 2007. [Online]. Available: http://conferences.sigcomm.org/hotnets/2007/papers/hotnets6-final131.pdf
[16] E. N. Gilbert, "Capacity of a burst-noise channel," *Bell Syst. Tech. J.*, vol. 39, no. 5, pp. 1253–1265, 1960.

[17] P. Guo, J. Cao, K. Zhang, and X. Liu, "Enhancing zigbee throughput under wifi interference using real-time adaptive coding," in *Proc. INFOCOM*, 2014, pp. 2858–2866.
[18] S. Guo, S. M. Kim, T. Zhu, Y. Gu, and T. He, "Correlated flooding in low-duty-cycle wireless sensor networks," in *Proc. ICNP*, 2011, pp. 383–392.
[19] P. Jacquet *et al.*, "Optimized link state routing protocol for ad hoc networks," in *Proc. IEEE INMIC*, Apr. 2001, pp. 62–68.
[20] J. Cartigny, F. Ingelrest, and D. Simplot, "RNG relay subset flooding protocols in mobile ad hoc networks," *Int. J. Found. Comput. Sci.*, vol. 14, no. 2, pp. 253–265, 2003.
[21] S. Ji, R. Beyah, and Z. Cai, "Snapshot/continuous data collection capacity for large-scale probabilistic wireless sensor networks," in *Proc. INFOCOM*, 2012, pp. 1035–1043.
[22] D. B. Johnson and D. A. Maltz, "Dynamic source routing in ad hoc wireless networks," in *Mobile Computing*. Norwell, MA, USA: Kluwer, 1996, pp. 153–181.
[23] S. Katti, H. Rahul, W. Hu, D. Katabi, M. Médard, and J. Crowcroft, "XORs in the air: Practical wireless network coding," in *Proc. ACM SIGCOMM*, 2006, pp. 243–254.
[24] A. Khreishah, I. M. Khalil, and J. Wu, "Distributed network coding-based opportunistic routing for multicast," in *Proc. MobiHoc*, 2012, pp. 115–124.
[25] S. M. Kim, S. Wang, and T. He, "cetx: Incorporating spatiotemporal correlation for better wireless networking," in *Proc. SenSys*, 2015, pp. 323–336.
[26] S. M. Kim, S. Wang, and T. He, "Exploiting causes and effects of wireless link correlation for better performance," in *Proc. 34th IEEE Conf. Comput. Commun. (INFOCOM)*, Jun. 2015, pp. 379–387.
[27] C. E. Koksal and H. Balakrishnan, "Quality-aware routing metrics for time-varying wireless mesh networks," *IEEE J. Sel. Areas Commun.*, vol. 24, no. 11, pp. 1984–1994, Nov. 2006.
[28] E. L. Li, R. Ramjee, M. M. Buddhikot, and S. C. Miller, "Network coding-based broadcast in mobile ad-hoc networks," in *Proc. INFOCOM*, 2007, pp. 1739–1747.
[29] H. Lim and C. Kim, "Flooding in wireless ad hoc networks," *Comput. Commun. J.*, vol. 24, nos. 3–4, pp. 353–363, 2001.
[30] T. Liu and A. Cerpa, "Foresee (4C): Wireless link prediction using link features," in *Proc. IPSN*, 2011, pp. 294–305.
[31] T. Liu and A. Cerpa, "Talent: Temporal adaptive link estimator with no training," in *Proc. SenSys*, 2012, pp. 253–266.
[32] W. Lou and J. Wu, "On reducing broadcast redundancy in ad hoc wireless networks," *IEEE Trans. Mobile Comput.*, vol. 1, no. 2, pp. 111–122, Feb. 2002.
[33] S. Pattem, B. Krishnamachari, and R. Govindan, "The impact of spatial correlation on routing with compression in wireless sensor networks," *ACM Trans. Sensor Netw.*, vol. 4, no. 4, p. 24, 2008.
[34] J. Polastre, J. Hill, and D. Culler, "Versatile low power media access for wireless sensor networks," in *Proc. SenSys*, 2004, pp. 95–107.
[35] A. Qayyum, L. Viennot, and A. Laouiti, "Multipoint relaying for flooding broadcast messages in mobile wireless networks," in *Proc. HICSS*, 2002, pp. 3866–3875.
[36] I. Rhee, A. Warrier, M. Aia, and J. Min, "Z-mac: A hybrid mac for wireless sensor networks," in *Proc. SenSys*, 2005, pp. 511–524.
[37] K. Srinivasan, P. Dutta, A. Tavakoli, and P. Levis, "An empirical study of low-power wireless," *ACM Trans. Sensor Netw.*, vol. 6, no. 2, pp. 1–16, 2010.
[38] K. Srinivasan *et al.*, "The κ factor: Inferring protocol performance using inter-link reception correlation," in *Proc. MobiCom*, 2010, pp. 317–328.
[39] K. Srinivasan, M. A. Kazandjieva, S. Agarwal, and P. Levis, "The β-factor: Measuring wireless link burstiness," in *Proc. SenSys*, 2008, pp. 29–42.
[40] J. Tang, G. Xue, C. Chandler, and W. Zhang, "Interference-aware routing in multihop wireless networks using directional antennas," in *Proc. INFOCOM*, 2005, pp. 751–760.
[41] P.-J. Wan, Z. Wang, H. Du, S. C.-H. Huang, and Z. Wan, "First-fit scheduling for beaconing in multihop wireless networks," in *Proc. INFOCOM*, 2010, pp. 1–8.
[42] S. Wang *et al.*, "Link-correlation-aware opportunistic routing in wireless networks," *IEEE Trans. Wireless Commun.*, vol. 14, no. 1, pp. 47–56, Jan. 2015.
[43] S. Wang, S. M. Kim, Y. Liu, G. Tan, and T. He, "Corlayer: A transparent link correlation layer for energy efficient broadcast," in *Proc. MobiCom*, 2013, pp. 51–62.
[44] S. Wang, S. M. Kim, Z. Yin, and T. He, "Correlated coding: Efficient network coding under correlated unreliable wireless links," in *Proc. IEEE ICNP*, Apr. 2014, pp. 433–444.
[45] *IEEE Standard Part 11: Wireless LAN Medium Access Control (MAC) and Physical Layer (PHY) Specifications*, IEEE Standard 802.11-2012, Wireless LAN Working Group, Mar. 2012.
[46] *IEEE Standard Part 15.4: Low-Rate Wireless Personal Area Networks (LR-WPANS)*, IEEE Standard 802.15.4-2011, Wireless Personal Area Network (WPAN) Working Group, Sep. 2011.
[47] A. Woo, T. Tong, and D. E. Culler, "Taming the underlying challenges of reliable multihop routing in sensor networks," in *Proc. ACM SenSys*, 2003, pp. 14–27.
[48] J. Wu and W. Lou, "Forward-node-set-based broadcast in clustered mobile ad hoc networks," *Wireless Commun. Mobile Comput.*, vol. 3, no. 2, pp. 155–173, May 2003.
[49] J. Wu, M. Lu, and F. Li, "Utility-based opportunistic routing in multi-hop wireless networks," in *Proc. ICDCS*, 2008, pp. 1–6.
[50] G. Xing, M. Li, H. Luo, and X. Jia, "Dynamic multiresolution data dissemination in wireless sensor networks," *IEEE Trans. Mobile Comput.*, vol. 8, no. 9, pp. 1205–1220, Sep. 2009.
[51] W. Ye, J. Heidemann, and D. Estrin, "Medium access control with coordinated, adaptive sleeping for wireless sensor networks," *IEEE/ACM Trans. Netw.*, vol. 12, no. 3, pp. 493–506, Jun. 2003.
[52] W. Ye, F. Silva, and J. Heidemann, "Ultra-low duty cycle mac with scheduled channel polling," in *Proc. SenSys*, 2006, pp. 321–334.
[53] Z. Zhao *et al.*, "Modeling link correlation in low-power wireless networks," in *Proc. INFOCOM*, 2015, pp. 990–998.

Song Min Kim received the B.E. and M.E. degrees from the Department of Electrical and Computer Engineering, Korea University, in 2007 and 2009, respectively, and the Ph.D. degree from the Department of Computer Science and Engineering, University of Minnesota, in 2016. He is currently an Assistant Professor with the Department of Computer Science, George Mason University, VA, USA. His research interests include wireless and low-power embedded networks, mobile computing, Internet of Things, and cyber-physical systems. He particularly enjoy designs motivated by analysis on extensive experimental data, followed by real-world implementations to validate their impact in practice.

Shuai Wang received the B.S. and M.S. degrees from the Huazhong University of Science and Technology, China, and the Ph.D. degree from the Department of Computer Science and Engineering, University of Minnesota, in 2017. He currently holds a post-doctoral position with the Department of Computer Science and Engineering, University of Minnesota. His research interests include Internet of Things, mobile cyber physical systems, big data analytics for intelligent transportation systems, and wireless networks and sensors.

Tian He received the Ph.D. degree from the University of Virginia, VA, USA, under the supervision of Prof. J. A. Stankovic. He is currently a Full Professor with the Department of Computer Science and Engineering, University of Minnesota-Twin Cities. He has authored and co-authored over 200 papers in premier network journals and conferences with over 20 000 citations (h-index 59). His research includes wireless sensor networks, cyber-physical systems, intelligent transportation systems, real-time embedded systems, and distributed systems, supported by the National Science Foundation, IBM, Microsoft, and other agencies. He was a recipient of the NSF CAREER Award in 2009, the McKnight Land-Grant Chaired Professorship in 2011, the George W. Taylor Distinguished Research Award in 2015, the China NSF Outstanding Overseas Young Researcher I and II in 2012 and 2016, and five best paper awards in international conferences. He has served a few general/program chair positions in international conferences and on many program committees and also has been an Editorial Board Member of six international journals including the *ACM Transactions on Sensor Networks* and the IEEE TRANSACTIONS ON COMPUTERS.